Design Automation for Paper Microfluidics with Passive Flow Substrates

Joshua Potter[1], William Grover[2], Philip Brisk[1]
[1]Department of Computer Science and Engineering, [2] Department of Bioengineering
University of California, Riverside

ABSTRACT

This paper introduces a novel software framework to support automated development of paper-based microfluidic devices. Compared to existing lab-on-a-chip technologies, paper-based microfluidics differs in terms of substrate technologies and point-of-care usage across a wide variety environmental conditions. This paper addresses the contexts in which the software can address these challenges and presents several initial case studies that demonstrate the capabilities of the framework to produce workable and usable paper microfluidic devices.

CCS Concepts

•**Applied computing** → *Computer-aided design; Health care information systems;*

Keywords

Paper Microfluidics; Design Automation; Capillary; Passive Flow; Assay

1. INTRODUCTION

Each year, approximately 5 million people worldwide die from AIDS and tuberculosis, another 4.3 million die from respiratory infections, around 2.9 million die from enteric infections, and about 1 million die from malaria. Virtually all of these deaths occur in developing countries [5]. Diagnostics suitable for use in resource-limited settings have the potential to save millions of lives each year and improve the quality of life worldwide. Even in first-world countries, a lack of adequate diagnostics makes healthcare less efficient and a financial burden to society. Better point-of-care diagnostics can play a crucial role in health care by providing doctors with rapid diagnoses, enabling treatment to begin while the patient is still at the hospital. This reduces the number of hospital visits and helps patients recover faster; however, developing diagnostics for successful use in resource-limited and point-of-care settings is a formidable challenge.

1.1 Motivation

The *World Health Organization (WHO)* recently defined the *ASSURED* criteria, a set of characteristics that are essential for diagnostics in both resource-limited and point-of-care applications [5]. *ASSURED* diagnostics must be:

A: Affordable by those at risk of infection
S: Sensitive (few false-negatives)
S: Specific (few false-positives)
U: User-friendly (requiring minimal training)
R: Rapid (treatment at first visit) and robust
  (no refrigerated storage)
E: Equipment-free (no additional equipment needed for use)
D: Delivered to those who need it (small and portable)

Paper microfluidic diagnostic devices satisfy all seven of the *ASSURED* criteria [7]. In contrast to expensive conventional laboratory-scale instruments or integrated laboratories-on-a-chip, paper microfluidic devices are made from inexpensive materials, are easily mass-produced, and exhibit the high sensitivity and specificity that are hallmarks of more complicated microfluidic technologies. Meanwhile their simple operation is user-friendly and easy to use (consider the simplicity of the home pregnancy test strip).

By operating on extremely small sample volumes (nanoliters to microliters), paper microfluidic diagnostics can be very rapid. Using dehydrated reagents immobilized in the paper eliminates the need for refrigeration and making them more robust than laboratories-on-a-chip or laboratory-scale instruments. Paper microfluidics often integrate the readout into the paper itself (e.g., as a color change), eliminating the need for equipment like microscopes or sensors and makes paper microfluidics essentially equipment-free; in fact, recent work has shown that cellular phone cameras can provide effective readout capabilities for paper microfluidics. Being small and disposable, paper microfluidic devices can easily be delivered to doctors in the field and stocked at the point-of-care. As such, these devices are poised to proliferate as healthcare diagnostic solutions throughout the world.

1.2 Current Paper Microfluidic Design Practices

Despite the aforementioned advantages, designing, testing, and validating paper microfluidic diagnostics remains a significant hurdle, as the task is presently done by hand using software such as AutoCAD® or Adobe Illustrator®. Each design is essentially a "hard-coded" ASPMD (application-specific paper microfluidic device; analogous to an ASIC).

Although paper microfluidic devices are one-time use and disposable, during the development phase, researchers must create multiple variations to compare design performance and accuracy, and possibly to adapt the device for use in varying environmental conditions. Under the current design paradigm, the researcher would need to hand-design each variation, which is time-consuming, labor-intensive and prone to inaccuracy. These issues also limit the potential complexity of the biochemical assays (step-by-step chemical reactions) that a paper microfluidic device can realistically be designed to perform.

1.3 Traditional Circuits vs. Passive Flow Devices

Although there are many parallels between traditional circuit design and the proposed passive-flow technologies, the fundamental difficulties stem from the differences between electricity and fluids. When working with electricity, our design concerns stem from resistance, voltage, amperage, and heat. As long as we complete a circuit, the electrons will get there eventually.

When dealing with fluids, we have similar concerns when it comes to resistance to flow, capacity of flow and rate of flow. However additional concerns related to fluid dynamics include gravitational effects, fluid surface tension alongside substrate resistance, and finally, a limited amount of fluid to perform the process under test. Further complicating placement and routing, locations and distances are not necessarily discrete as successful device and layout generation may need fractional modification, therefore we have a continuous range of viable locations.

1.4 Contribution

This paper presents a software framework created by the authors intended to assist developers to design new paper microfluidic devices. Developers can use the framework to prototype and test new designs, which includes varying the underlying substrates and experimenting with passive flow networks. The framework also provides the capability to reliably reproduce devices streamlined for in-situ fabrication and to provide tools for testing and analysis of the designs; this, in turn, informs the alteration and rapid prototyping of design variations, helping to account for test results, environmental conditions, impact on physical substrates and fluids, and accuracy under test.

2. DESIGN AUTOMATION FRAMEWORK

Fig.1 provides an overview of the framework. It includes a library of paper microfluidic components, which can be rapidly assembled into netlists which form new devices. Once the netlist is assembled, the framework renders the device using established file formats (*PDF*, *DXF*, *SVG*). We now introduce the framework's operation from the bottom-up.

2.1 Technical Details

The framework has been developed using C++ 11 in the Ubuntu v14.0.4 Linux distribution. Code is compiled using GCC v5.1 compiler via a *makefile* utilizing multi-threading, `-Wall` and `-Werror` flags. The programs and libraries are constructed to be platform-independent as much as possible, performing file I/O and other platform-specific tasks in individual libraries. As of this publication, the application is command-line only.
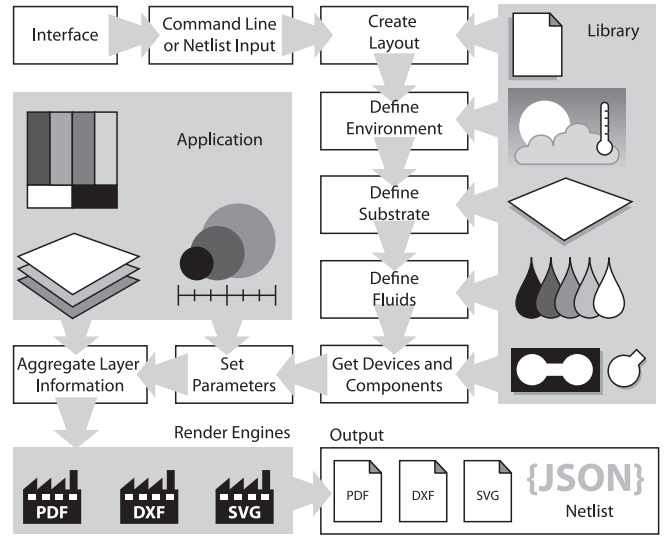

Figure 1: Framework overview

2.2 Segments, Paths, and Primitives

Segments, *paths*, and *primitives* refer to the elemental geometric shapes that can be printed onto a paper substrate. A segment is a Bezier curve, featuring source and sink coordinates that indicate a direction of drawing when rendered by the framework. The source and sink have handle coordinates that define the curve. If the handle coordinates are the same as the source and sink coordinates, then the curve degenerates to a line segment (Fig.2(a)) otherwise, they form a curve (Fig.2(b)).

Paths are constructed by concatenating multiple segments (Fig.2(c)). Primitives are closed paths, representing geometric shapes such as quadrilaterals, circles, ellipses, and polygons (Fig.2(d)). Union and intersection operations applied to Primitives can form complex shapes and Primitives with negative space (Fig.2(e)). The *Zero-sum Winding Rule* [2] can identify overlapping and negative spaces to determine the underlying paths that characterize the final shape.

2.3 Components and Devices

A *component* is a dynamically generated, re-usable object whose geometry is defined by one or more primitives, coupled with its functionality in terms of fluidic actions and abstract dynamics, such as mixing, transport, timing, etc.

A *device* consists of at least one or more components that encapsulate the desired actions and parameters needed to characterize biochemical behavior as described in the assay protocols. Individual components may be scaled or rotated
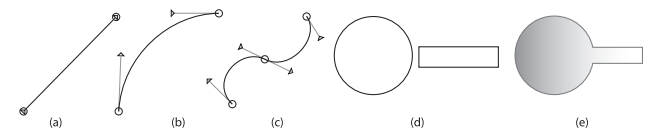

Figure 2: a) line segment, b) curve segment; c) a path constructed from two curve segments; d) a circle and a polygon primitive constructed from curve and straight segments; e) a component formed from multiple primitives.

as needed. Large devices may be specified hierarchically in terms of smaller devices, facilitating composition of multiple assays, either in sequence or in parallel.

2.4 Parameterization

The framework supports *parameterized components and devices*; for example, a straight fluid transport channel can be characterized in terms of its length and width. The device designer can then iterate over multiple versions, for example, to assess behavior of an assay under various loads, conditions, configurations, etc. This can be automated via dynamic drawing based on user-specified parameters. As the designer varies parameter values, the software adjusts and re-renders the component or device as needed.

2.5 Substrates and Substances

It is necessary to understand the properties of both the physical materials that the fluids that are expected to flow through it. The *substrate* abstracts the production of the output to individual pages (for printing) or other options (e.g., computer controlled-paper cutters). It encapsulates physical properties of materials, such as dimensions, margins, output area, expected flow rate, and fluid capacities. Attributes such as base flow rate for a given substrate can be used to calculate flow and dispersion times which can then determine expected execution time, timing variability, fluid consumption, and the probability of successful assay completion. Paper dimensions can be specified including margin size, along with mean flow rate for a fluid to travel within the substrate.

The *substance* encapsulates the physical characteristics of the various fluids, reagents, solutes, flow rates given a particular environment, etc., which are used to evaluate assay feasibility and accuracy, given a substrate.

2.6 Registries

Each device or component has a *registry*, which tracks and resolves the substrates onto which it will be printed. When two components or devices are merged, their registries are merged and reconciled to determine if the substrates and layers are compatible; if not, the device cannot be fabricated. If the device is feasible, a *layer registry* is built to determine which primitives, components, and devices will be printed on each layer. When appropriate, duplicates may be eliminated and components may be transferred from one layer to another, if needed. This reconciliation process produces a distilled list of substrates which the user can then verify for correctness.

2.7 Layouts

Paper dimensions can be specified including margin size, along with mean flow rate for a fluid to travel within the substrate. The *layout* represents the context in which a paper-based biochemical assay operate, including environmental information, substances and substrates, and the base units of measurement. The layout contains the netlist representation of each device, as well as its layer registry.

2.8 Scale and Color

Scale and *color* are application-level attributes that speak to the accuracy of components and may define the basic operating modes of a device. Scale refers to units of measurement (e.g., *mm*-scale devices), including conversion between
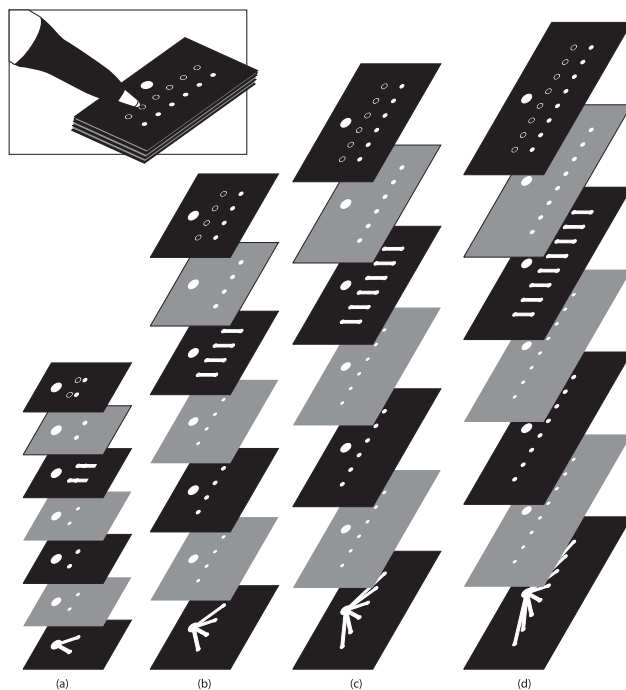

Figure 3: Parameterized fMux designs with a) two channels; b) four channels; c) six channels; and d) eight channels

units. The default internal unit of measurement is millimeters. Storing and maintaining a metric standard minimizes rounding error accumulation and reduces measurement error that can occur when multiple conversions between non-metric measurements cascade. The notion of color includes standard four to six color inks as well as non-ink materials such as wax or metallic ink for printing.

2.9 Environment

The *environment* provides measurements that may influence assay performance and accuracy, such as temperature, barometric pressure, and humidity; this allows designers to characterize the environmental conditions under which a device will properly operate. For example, should a warm temperature prolong flow rates, then various channels and other components should be shortened to maintain the expected runtime; in a humid environment, runtime may increase or cause incorrect mixing. Thus, it may be necessary to produce a general family of devices that are capable of executing one assay under different environmental conditions.

2.10 Rendering Engines

The framework's initial rendering engine outputs the PDF format, which is ubiquitous, and supports vector graphics with high resolution output; in practice, the print or output device, not the PDF format, will limit the achievable resolution of our framework. PDF is platform independent, which simplifies distribution of device designs and enhances reproducibility.

The second rendering engine targets AutoCAD's DXF file format, which has been a stable of computer-aided design (CAD) for decades. The DXF is a platform-agnostic drawing technology that can produce highly accurate vector
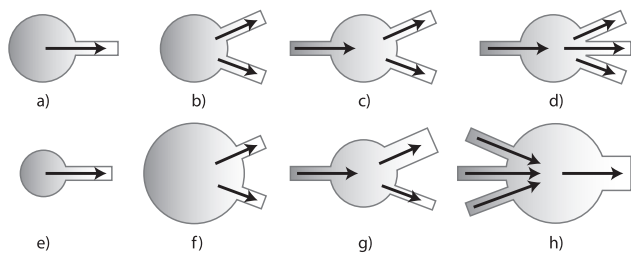
Figure 4: Well and channel components in 8 configurations: a) 1-out; b) 2-out; c) 1-in, 2-out; d) 1-in, 3-out; e) reduced well size with 1-out; f) increased well size with 2-out; g) 1-in, 2-out with channels of varying width; and h) increased well size with 3-in (narrow width), 1-out (wide width).

Figure 5: a) Raceway Calibration Device; b) Bullseye Calibration Device.

drawings. Due to the ubiquity of AutoCAD in computer-controlled machining (CNC) applications, the DXF format is compatible with cutting and pen-based drawing devices.

The last rendering engine targets W3C's Scalable Vector Graphics (SVG) format, an XML-based platform-agnostic file format. As SVG is widely used for web content, we expect to use this engine to distribute images primarily rendered for visual display and scientific dissemination.

3. CASE STUDIES

We briefly summarize a set of successful case studies which demonstrate that our framework can be used to print a variety of useful parameterizable components and devices. These case studies validate the practical usability of the framework, along with its basic capabilities.

3.1 Fluidic Multiplexers

We used the framework to reproduce a *fluidic multiplexer (fMux)* [6] (Fig.3), which is constructed from multiple layers of paper and tape. The user "programs" the fMux by squeezing the layers together at pre-specified locations (buttons) on the top layer, connecting two passive flow substrates; the tape layer ensures that each button remains pressed (i.e., the two passive flow substrates remain in contact) after compression.

The user can program a K:1 fMux so that any subset of K input fluids will merge and mix (by passive diffusion) at the fMux output. Parameterization allows the design to generate fMuxes with any desired number of inputs; the user may also adjust the fMux dimensions, channel length, and well size. The framework then draws the fMux channels algorithmically using the rendering engine.

3.2 Channel and Well Components

Channels and wells (Fig.4) can be parameterized to change dimensions, capacities, orientations, and signal counts.

A *channel* is specified by its source and sink coordinates, along with its width; it may also be specified as a vector with a source coordinate, angle, length, and width. The framework can assess the impact of channel design parameters on issues such as assay execution time, reagent consumption, etc.

A *well* is a circular region that contains one or more fluids; the primary parameter of interest is its radius. Using the framework, we produced two calibration devices that cap-
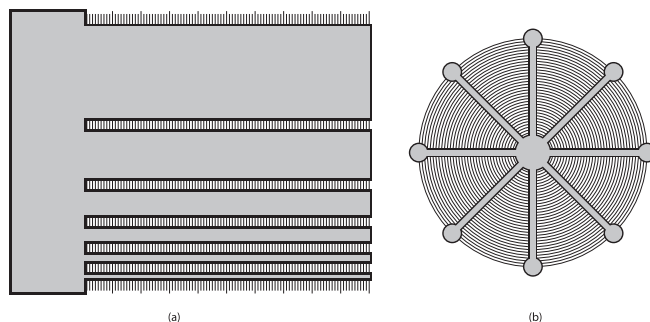
ture performance data across varying environmental conditions. These devices can enhance reproducibility of scientific findings across a variety of external conditions which are often beyond the control of the practitioners.

3.3 Calibration Devices

The Raceway Calibration Device (Fig.5(a)) comprises a varying number of fixed-length lanes (channel segments) with varying width. The Raceway allows a researcher to compare fluid transport velocities over time, enabling characterization of dispersion rates. Running multiple "races" using a median benchmark fluid under fixed environmental conditions will enable a researcher to characterize the +/- margin of the substrate with a high degree of confidence.

The Bullseye Calibration Device (Fig.5(b)) allows for lanes to be specified at various angles in a radial distribution around a central source or sink. It includes a measurement scale that expands out from the central point in concentric marks giving appearance of a bullseye target. Paper substrates may exhibit a flow orientation as a result of manufacturing processes; unlike the Raceway, the Bullseye device allows for the calibration process to take the flow orientation into account, as it may influence accuracy and performance.

Once the calibration profiles are obtained, they may be incorporated into the layout of a device, especially when tuning the device for specific environmental conditions. We anticipate that this will increase accuracy, reproducibility, and efficiency in terms of time and material utilization, both in laboratory and point-of-care settings.

4. EXPERIMENTAL RESULTS

This section summarizes the experimental setup, preliminary tests performed, observed difficulties, and solutions and processes that were develoepd to mitigate those difficulties. The reported experiments 1) determined a reliable width of the printed barrier walls to contain fluid transfer; and 2) assessed the reliability and replicability of experiments performed with devices produced by the software.

4.1 Experimental Setup

Microfluidic layouts generated by the framework for testing were printed using a Xerox ColorQube 8570DN wax-based ink printer connected via USB cable directly to a PC used for development. The printer driver's output resolution was set to 1200 dots-per-inch (dpi) with zero-scaling during output to maintain accurate rendering of files to substrates.

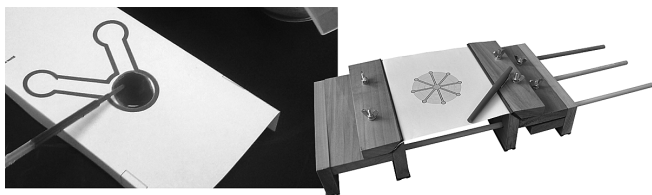The wax printer delivers color solid wax "inks" to paper by

Figure 6: On the left, the first tests when creating wax-based channels for fluid flow. On the right, the test rig isolates the material and fluids from contact while under test.
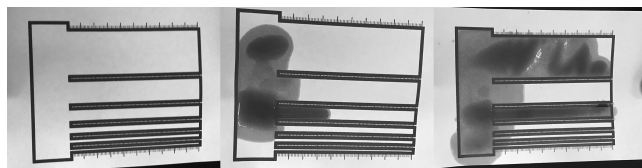

Figure 7: Simple experiment to test the Raceway Calibration device's containment efficacy. From left, @t=0 min, prior to dispensing fluid, @t=1 min, fluid contained by $2mm$ borders, @t=2 min, fluid flows beyond borders due to improper handling of substrate.

activating an internal heating element, which melts the wax to a fluid state before depositing it on the surface material, where it rapidly cools before being ejected from the printer. Although the wax ink is hydrophobic, it resides on top of the paper, so fluids delivered to the substrate at this stage would penetrate beneath the ink, bypassing the desired barried on the surface. Passing the printed page over a heating element re-melts the wax, which then flows into the substrate to create the desired hydrophobic barrier.

A $100 - 1000\mu$L-range pipette was used for measurement and delivery of a solution of filtered water colored with a standard food colorant. LabNerd® filter paper cut to $7.875'' \times 4.875''$ served as the substrate.

4.2 Test Rig

In our initial tests, the ends of the paper were folded over to create a rigid support (Fig.6, Left), which elevated the test area, but did not create a taut and level surface; consequently, when liquid was applied to the substrate, undesired flow would occur. Even with a 2 mm border to contain liquid flow to the desired regions, the uneven surface caused warping and uncontrolled and transport (Figure 7). Our solution was to design and construct a test rig which isolates the substrates from other surfaces and maintains a level flow surface such to ensure that fluid is not under the influence of gravity while under test (Fig.6, Right). Results for subsequent experiments are reported using the test rig.

4.3 Fluid Containment

The goal of this experiment was to determine a border width for reliable fluid containment for channels and wells under test. We ran several passes on the Raceway and Bullseye calibration devices using fluid volumes of 1000μL, 500μL, 300μL, and 250μL. For the Raceway device, 500μL of fluid caused a failure in the reservoir section, while 300μL reliably filled a Bullseye device with a $40mm$ radius. Subsequent experiments to test fluid containment were performed on the Bullseye device using 300μL of fluid with border widths of $0.5mm$, $1.0mm$, $1.5mm$, and $2.0mm$.

As shown in Figure 8, border widths of $0.5mm$ and $1.0mm$ failed to contain the fluid delivered to the source location in the center with fluid seeping through the channel barriers. The $1.5mm$ width performed better, but exhibited a failure at the $30mm$ mark (as indicated by the arrow in Figure 8), but otherwise contained most of the fluid. The $2mm$ width reliably contained the 300μL fluid, which was delivered to the source and then flowed to each of the eight sinks. In principle, this will allow us to test flow rates over varying device sizes; additional testing will attempt to determine the relationship (if any) of fluid volume to barrier size.

4.4 Flow Characterization and Replicability

We fabricated thirty $40mm$-radius Bullseye devices, two per sheet, and pipetted 200 μL of fluid to the source. For each device, we measured the fastest and slowest times at which fluid reached one of the eight $40mm$ sinks. The results (Table 1) suggest exceptionally high variability: fluid transport time ranged from $144-560$ s, with a median of 427 s and a standard deviation of 76.54 s. The primary cause for the variability turned out to be inconsistent pipetting, which, in turn, led to inconsistent fluid transport. Taken in its proper context, this variability is likely to manifest itself in real-world use cases, where the user of a paper-based diagnostic is a layperson, not a trained healthcare professional. Thus, there is likely to be similar high variability between different users of otherwise identical devices. Thus, experiments such as this can provide, at a bare minimum, upper and lower bounds on the time required to execute a biological assay on a paper microfluidic device; this type of information can and should be included in experimental protocols to ensure that the user has a realistic estimate of how long to wait before trying to interpret the results.

Table 1: Maximum and minimum fluid transport times recorded using the Bullseye device with eight $3mm$ sinks and $40mm$ long channels, having a $2mm$ border width, with 200μL fluid delivered to the source.

Trial	MIN	MAX	Trial	MIN	MAX
1	488 s	560 s	16	392 s	440 s
2	468 s	480 s	17	396 s	428 s
3	432 s	462 s	18	354 s	414 s
4	416 s	446 s	19	144 s	157 s
5	374 s	456 s	20	157 s	384 s
6	374 s	432 s	21	334 s	468 s
7	450 s	504 s	22	426 s	468 s
8	458 s	488 s	23	368 s	440 s
9	372 s	372 s	24	438 s	438 s
10	358 s	358 s	25	360 s	398 s
11	392 s	432 s	26	338 s	376 s
12	406 s	406 s	27	438 s	476 s
13	376 s	480 s	28	442 s	462 s
14	408 s	482 s	29	328 s	446 s
15	452 s	452 s	30	314 s	422 s

5. RELATED WORK

To the best of our knowledge, there has been no prior work on design automation for paper microfluidic devices
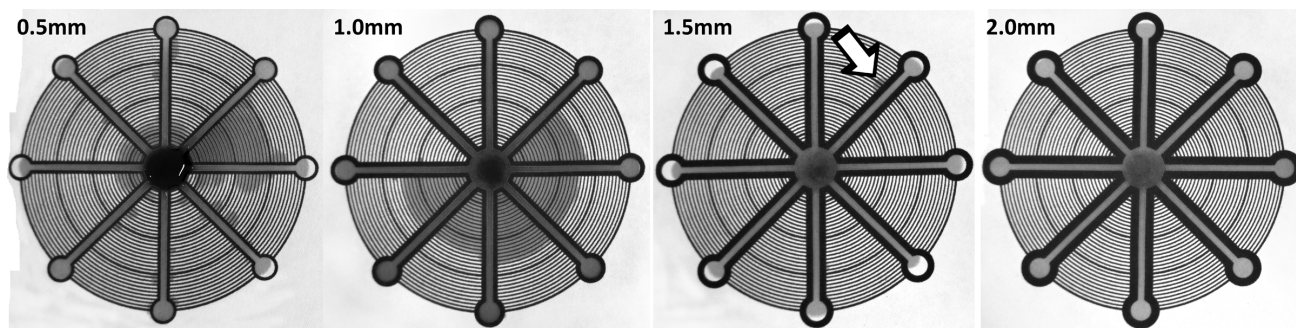
Figure 8: Fluid containment experiment to determine reliable border thickness for fluid containment. Note: photos had contrast adjusted to more clearly show fluid location)

based on passive flow substrates; many individual devices, designed manually, have been reported [4, 5]. There has been some prior work on physical design and droplet routing [9], control pin optimization [8] and test [10] for paper-based electrowetting devices patterned using conductive ink [1, 3]; these devices transport liquid through the application of high-voltage electrostatic forces, as opposed to passive capillary flow. In principle, our framework could be used to print the conductive ink patterns on the paper. In the future, we may try to use our framework to build paper devices that integrate electrowetting circuitry with passive flow substrates.

6. CONCLUSION AND FUTURE WORK

Paper-based microfluidics provide portable laboratory tests without expensive actuation equipment. Paper microfluidics replaces externally-actuated pumps and high-voltage-driven electrodes with low-cost wicking materials, thereby reducing the cost of fabricating new devices and performing diagnostic tests; however, this does not automatically imply a reduction in complexity of the design process.

To address these concerns, we have introduced a software framework that can simplify and automate the design process. Although we do not expect to attain end-to-end push-button automation any time soon, we do believe that this software can help device designers deal with many of the most pressing challenges.

Future work will focus on integrating design automation algorithms such as placement and routing of paper microfluidic components and fluid channels as well as conduct further exploration of the physical characteristics of both substrates and fluids used in biological assays to create profiles which will inform those algorithms to help determine both successful placement of components and viability of routing solutions of layouts.

We have highlighted challenges associated with paper substrate heterogeneity and variations in environmental conditions: as paper microfluidic devices are expected to yield consumer-facing products, they are unlikely to be used in high controlled laboratory settings.

ACKNOWLEDGMENTS

7. REFERENCES

[1] A. Abadian and S. Jafarabadi-Ashtiani. Paper-based digital microfluidics. *Microfluidics and Nanofluidics*, 16(5):989–995, 2014.

[2] A. Jacobson, L. Kavan, and O. Sorkine-Hornung. Robust inside-outside segmentation using generalized winding numbers. *ACM Transactions on Graphics (TOG)*, 32(4):33, 2013.

[3] H. Ko, J. Lee, Y. Kim, B. Lee, C.-H. Jung, J.-H. Choi, O.-S. Kwon, and K. Shin. Active digital microfluidic paper chips with inkjet-printed patterned electrodes. *Advanced Materials*, 26(15):2335–2340, 2014.

[4] A. M. López-Marzo and A. Merkoçi. Paper-based sensors and assays: a success of the engineering design and the convergence of knowledge areas. *Lab-on-a-Chip*, 16(17):3150–3176, 2016.

[5] D. Mabey, R. W. Peeling, A. Ustianowski, and M. D. Perkins. Tropical infectious diseases: diagnostics for the developing world. *Nature Reviews Microbiology*, 2(3):231–240, 2004.

[6] A. W. Martinez, S. T. Phillips, Z. Nie, C.-M. Cheng, E. Carrilho, B. J. Wiley, and G. M. Whitesides. Programmable diagnostic devices made from paper and tape. *Lab-on-a-Chip*, 10(19):2499–2504, 2010.

[7] A. W. Martinez, S. T. Phillips, G. M. Whitesides, and E. Carrilho. Diagnostics for the developing world: Microfluidic paper-based analytical devices. *Analytical Chemistry*, 82(1):3–10, 2010. PMID: 20000334.

[8] Q. Wang, Z. Li, H. Cheong, O.-S. Kwon, H. Yao, T.-Y. Ho, K. Shin, B. Li, U. Schlichtmann, and Y. Cai. Control-fluidic codesign for paper-based digital microfluidic biochips. In *Proceedings of the 35th International Conference on Computer-Aided Design*, pages 103:1–103:8, 2016.

[9] S.-J. Wang, K. S.-M. Li, and T.-Y. Ho. Congestion-and timing-driven droplet routing for pin-constrained paper-based microfluidic biochips. In *Proceedings of the 21st Asia and South Pacific Design Automation Conference*, pages 593–598, 2016.

[10] S.-J. Wang, K. S.-M. Li, and T.-Y. Ho. Test and diagnosis of paper-based microfluidic biochips. In *Proceedings of the 4th IEEE VLSI Test Symposium*, pages 1–6, 2016.